Fracture 1977, Volume 3, ICF4, Waterloo, Canada, June 19 - 24, 1977

SUDDEN TWISTING OF A PENNY-SHAPED CRACK IN A FINITE ELASTIC CYLINDER

E. P. Chen*

INTRODUCTION

In the field of fracture dynamics, much of the previous investigation have been concerned with the determination of the nature of the dynamic stresses near a crack in a body of infinite extent. For axisymmetric geometry, a number of papers [1-5] have discussed the inertia effect on the dynamic stress intensity factors. However, due to the mathematical complexities involved, the interaction between scattered waves by a penny-shaped crack and reflected waves from finite boundaries has not been considered.

In this paper, the torsional impact response of a penny-shaped crack in a finite elastic cylinder is considered. Application of the Laplace and Hankel transforms reduces the problem to the solution of a pair of dual integral equations. These equations are solved by using an integral transform technique and the result is expressed in terms of a Fredholm integral equation of the second kind. The time dependence is recovered by applying the Laplace inversion theorem. Numerical solutions are obtained for the amplitude of the local stress field near the crack; that is, the dynamic stress intensity factor. The influence of the interaction between scattered waves by the crack and reflected waves from the boundaries are discussed. Although only stress-free cylinder surface condition is considered, other boundary conditions can be treated in a similar manner without additional difficulties.

PROBLEM FORMULATION

Let the axis of an elastic cylinder coincide with the z axis of a cylindrical polar coordinate system (r,θ,z). The cylinder is made of a homogeneous and isotropic material and its radius is denoted b. A penny-shaped crack of radius a is lying on the plane z=0 with its center at the origin of the coordinate axes. The geometry of the problem is shown in Figure 1.

The displacements in the r, θ and z directions are denoted, respectively, by u_r, u_θ and u_z. The cylinder is under the action of a rapidly applied torque such that the material particles experience only an angular displacement. Hence, u_r and u_z vanish throughout the body and from symmetry considerations, u_θ is a function of r, z and time t only. The displacement field can thus be written as

$$u_r = u_z = 0 \ , \ u_\theta = u_\theta(r,z,t) \tag{1}$$

*Lehigh University, Bethlehem, Pennsylvania, U.S.A.

Corresponding to equations (1), all stress components except $\tau_{r\theta}$ and $\tau_{\theta z}$ vanish and the shear stresses are given by the following expressions:

$$\tau_{r\theta}(r,z,t) = \mu \left(\frac{\partial u_\theta}{\partial r} - \frac{u_\theta}{r}\right) \tag{2}$$

$$\tau_{\theta z}(r,z,t) = \mu \frac{\partial u_\theta}{\partial z} \tag{3}$$

in which μ is the shear modulus of elasticity. Substituting equations (2) and (3) into the equations of motion of elasticity, it follows that two of them are identically satisfied and the remaining one renders

$$\frac{\partial^2 u_\theta}{\partial r^2} + \frac{1}{r}\frac{\partial u_\theta}{\partial r} - \frac{u_\theta}{r^2} + \frac{\partial^2 u_\theta}{\partial z^2} = \frac{1}{c_2^2}\frac{\partial^2 u_\theta}{\partial t^2} \tag{4}$$

The shear wave velocity c_2 is given by $c_2 = (\mu/\rho)^{1/2}$ with ρ being the mass density of the material.

The cylinder is assumed to be initially at rest. A torque T of magnitude $T = \pi b^4 \tau_o/(2a)$, with τ_o having the dimension of stress, is suddenly applied to the elastic body generating torsional waves normally incident on the crack. By the principle of superposition, the equivalent boundary conditions for which the wave passes across the crack plane at t=0 can be written as

$$\tau_{\theta z}(r,o,t) = -\tau_o\left(\frac{r}{a}\right)H(t), \quad 0<r<a \tag{5}$$

$$u_\theta(r,o,t) = 0, \quad r\geq a \tag{6}$$

In addition, the traction-free condition at the cylinder surface requires

$$\tau_{r\theta}(b,z,t) = 0 \tag{7}$$

Equation (4) is to be solved under the constraint of equations (5), (6) and (7).

Applying a Laplace transform pair

$$f^*(p) = \int_o^\infty f(t)e^{-pt}dt, \quad f(t) = \frac{1}{2\pi i}\int_{Br} f^*(p)e^{pt}dp \tag{8}$$

to equation (4) yields

$$\frac{\partial^2 u_\theta^*}{\partial r^2} + \frac{1}{r}\frac{\partial u_\theta^*}{\partial r} - \frac{u_\theta^*}{r^2} + \frac{\partial^2 u_\theta^*}{\partial z^2} = \frac{p^2}{c_2^2}u_\theta^* \tag{9}$$

For a finite cylinder, the solution to (9) may be written as

$$u_\theta^* = \int_o^\infty A(s,p,J_1(rs)e^{-\gamma z}ds + \int_o^\infty B(s,p)I_1(\gamma r)\sin(sz)ds \tag{10}$$

where J_n and I_n are, respectively, the nth order Bessel and modified Bessel function of the first kind. The function γ is given by

$$\gamma = \sqrt{s^2 + \frac{p^2}{c_2^2}} \tag{11}$$

Making use of equations (2), (10) and the Laplace transform of equations (5) and (6) renders a pair of dual integral equations:

$$\int_o^\infty \gamma A(s,p)J_1(rs)ds = \int_o^\infty sB(s,p)I_1(\gamma r)ds + \frac{\tau_o r}{\mu a p}, \quad r<a \tag{12}$$

$$\int_o^\infty A(s,p)J_1(rs)ds = 0, \quad r\geq a \tag{13}$$

The relationship between A(s,p) and B(s,p) is found, by taking Laplace and Fourier sine transforms on equation (7), as

$$\gamma B(s,p)I_2(\gamma b) = \frac{2}{\pi}s\int_o^\infty \frac{\eta A(\eta,p)J_2(b\eta)}{\eta^2+\gamma^2}d\eta \tag{14}$$

A solution to equations (12) and (13) satisfying equation (14) may be obtained by a procedure described in [5] and the result is

$$A(s,p) = \frac{\sqrt{2sa}}{\pi}\frac{2\tau_o a^2}{3\mu p}\int_0^1 \sqrt{\eta}\,\Phi^*(\eta,p)J_{3/2}(sa\eta)d\eta \tag{15}$$

where the function $\Phi^*(\eta,p)$ is governed by a Fredholm integral equation of the second kind:

$$\Phi^*(\xi,p) + \int_0^1 K(\xi,\eta,p)\Phi^*(\eta,p)d\eta = \xi^2 \tag{16}$$

The symmetric kernel $K(\xi,\eta,p)$ is defined by

$$K(\xi,\eta,p) = \sqrt{\xi\eta}\left\{\int_0^1 (\gamma'-s)J_{3/2}(\xi s)J_{3/2}(\eta s)ds - \frac{2}{\pi}\int_o^\infty \frac{s^2}{\gamma'}\frac{K_2(\gamma'\frac{b}{a})}{I_2(\gamma'\frac{b}{a})}I_{3/2}(\xi\gamma')I_{3/2}(\eta\gamma')ds\right\} \tag{17}$$

in which

$$\gamma' = \sqrt{s^2 + \frac{p^2a^2}{c_2^2}} \tag{18}$$

and K_2 is the second order modified Bessel function of the second kind.

NUMERICAL RESULTS AND DISCUSSION

Following the same procedures as in [3], the stresses local to the penny-shaped crack in the Laplace transform domain may be obtained as

$$\tau^*_{r\theta}(r_1,\theta_1,p) = -\frac{4}{3\pi}\tau_o\sqrt{a}\,\frac{\Phi^*(1,p)}{p}\,\frac{1}{\sqrt{2r_1}}\sin\frac{\theta_1}{2} + 0(r^o) \quad (19)$$

$$\tau^*_{\theta z}(r_1,\theta_1,p) = \frac{4}{3\pi}\tau_o\sqrt{a}\,\frac{\Phi^*(1,p)}{p}\,\frac{1}{\sqrt{2r_1}}\cos\frac{\theta_1}{2} + 0(r^o) \quad (20)$$

where r_1 and θ_1 are the polar coordinates centered at the crack border in the plane z=0. Applying the Laplace inversion theorem to equations (19) and (20) renders

$$\tau_{r\theta}(r_1,\theta_1,p) = -\frac{K_3(t)}{\sqrt{2r_1}}\sin\frac{\theta_1}{2} + 0(r^o) \quad (21)$$

$$\tau_{\theta z}(r_1,\theta_1,p) = \frac{K_3(t)}{\sqrt{2r_1}}\cos\frac{\theta_1}{2} + 0(r^o) \quad (22)$$

The dynamic stress intensity factor $k_3(t)$ is defined as

$$k_3(t) = \frac{4}{3\pi}\tau_o\sqrt{a}\,\frac{1}{2\pi i}\int_{Br}\frac{\Phi^*(1,p)}{p}e^{pt}dp \quad (23)$$

In order to obtain numerical values of $k_3(t)$, the Fredholm integral equation (16) is first solved on an electronic computer. Once Φ^* is determined, the dynamic stress intensity factor may be obtained by a numerical Laplace inversion scheme described in [3].

Note that by letting $p\to 0$, the solution presented here reduces to that for the corresponding static case of the same geometry. Figure 2 depicts the variation of the normalized static stress intensity factor $\bar{k}_3 = k_3/(4\tau_o\sqrt{a}/3\pi)$ versus the radius ratio a/b. It can be seen that as the ratio a/b is increased, the stress intensity factor also becomes higher. The rate of increase is very small when a/b is less than 0.5 and becomes significantly larger when a/b exceeds 0.5. This suggests that the effect of finite boundaries is serious only when the radius of the cylinder is less than two times of that of the penny-shaped crack.

The normalized dynamic stress intensity factor $\bar{k}_3(t)$ is plotted in Figure 3 against the time variable c_2t/a for various b/a ratios. The dynamic stress intensity factor increases quickly, reaching a peak, and then decreases in magnitude oscillating about the corresponding static value. This type of time dependence has also been observed in [3] for an infinite geometry problem. As b/a decreases, the peak value of $\bar{k}_3$ becomes larger and occurs at a later time. For b/a = 1.1, the interaction between inertia and finite geometry can increase the dynamic stress intensity factor by 65% over its corresponding static value in an infinite medium. Hence, it is obvious that this interaction effect is quite significant and cannot be ignored.

In summary, the interaction effect between scattered waves by a penny-shaped crack and reflected waves from finite boundaries on a cylinder under torsional impact has been determined. The dynamic stress intensity is found to be a function of time and the geometrical parameter b/a. The dynamic stress intensity factor reaches a peak very quickly and then decreases in magnitude oscillating about its corresponding static value. The peak value of the amplitude of the dynamic stresses is higher when the ratio b/a is reduced.

ACKNOWLEDGEMENTS

This work is part of a research program sponsored by the Army Research Office under Grant No. DAAG29-76-G-0091.

REFERENCES

1. SIH, G.C. and LOEBER, J.F., J. Acoust. Soc. America, 44, 1968, 1237.
2. SIH, G.C. and LOEBER, J.F., J. Acoust. Soc. America, 46, 1969, 711.
3. SIH, G.C. and EMBLEY, G.T., J. Appl. Mech., 39, 1972, 395.
4. EMBLEY, G.T. and SIH, G.C., Proceedings of the 12th Midwestern Mechanics Conference, Development in Mechanics, 6, 1972, 473.
5. KASSIR, M.K. and SIH, G.C., Three Dimensional Crack Problems, Volume 2, Mechanics of Fracture Series, edited by G.C. Sih, Noordhoff International Publishing Company, The Netherlands, 1975.

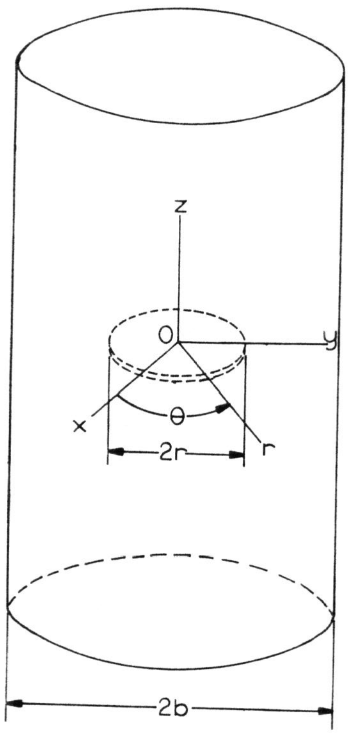

Figure 1   Finite cylinder containing a penny-shaped crack

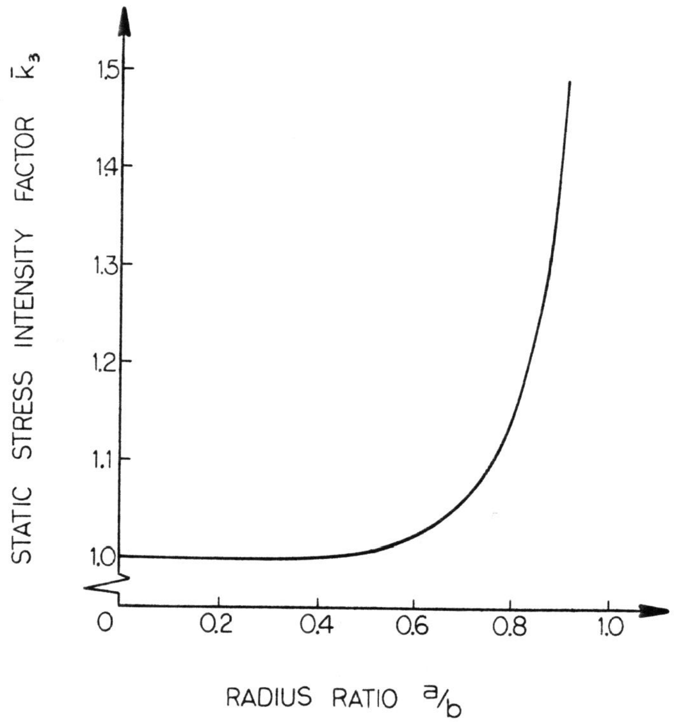

Figure 2   Normalized static stress intensity factor versus a/b

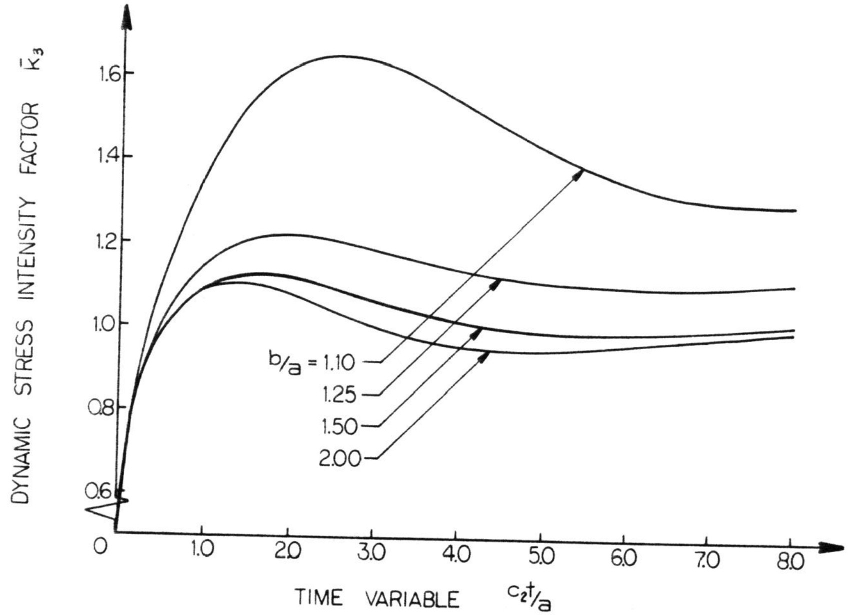

Figure 3 Normalized dynamic stress intensity factor versus time